

Bet-hedging against Demographic Variations

BingKan Xue¹ and Stanislas Leibler^{1,2}

¹*The Simons Center for Systems Biology, Institute for Advanced Study, Princeton, NJ 08540.*

²*Laboratory of Living Matter and Center for Studies in Physics and Biology,
The Rockefeller University, New York, NY 10065.*

Biological species have to cope with stochastic variations in both the external environment and the internal population dynamics. Theoretical studies and laboratory experiments suggest that population diversification could be an effective bet-hedging strategy for adaptation to temporally varying environments. Here we show that bet-hedging can also be effective against demographic fluctuations that cause extinction of local populations. A species can maximize its overall abundance in the long term by diversifying into coexisting subpopulations of both “fast-growing” and “better-surviving” individuals. Our model generalizes statistical physics models of birth-death processes to incorporate migration between multiple populations and variation of local environments. The results show that organisms can use bet-hedging as a common defense mechanism against different types of uncertainties in population growth.

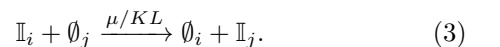
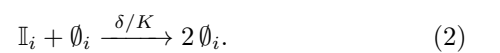
The growth of biological populations in nature is a stochastic process influenced by various kinds of uncertainties, including environmental and demographic fluctuations. Each kind of uncertainty could pose a potential risk to the survival of a species. During the course of evolution, those species that found ways to cope with uncertainties have generally been more successful and become relatively more abundant. A common theme in dealing with uncertainties is to “hedge the risks”. A population may exhibit diversified phenotypes as a means to hedging against environmental uncertainties [1, 2]: each phenotype may be favorable for a particular environmental condition but unsuitable for others. Since environmental variations are unpredictable, having multiple groups of individuals with different preadapted phenotypes ensures the survival of a certain subpopulation and thus the population as a whole. It is argued that such “bet-hedging” may have evolved as it increases the asymptotic growth rate of a population, thus helping the species to reach greater abundance in the long term (e.g., [3]).

On the other hand, due to the stochastic nature of birth and death processes, even in the absence of environmental variations, the growth of a population undergoes fluctuations in size. Such demographic fluctuations may cause a population to go extinct, which poses a significant risk especially for small populations, such as new colonies that are founded by a small number of individuals during range expansion. Could phenotypic diversification help to hedge against demographic uncertainties? To answer this question, it is inadequate to measure the evolutionary success of a species by the asymptotic growth rate. Indeed, the latter is usually calculated for a single population in the limit of an infinite population size, ignoring demographic fluctuations. In reality, populations are finite and often localized at their ecological habitats, such as bacteria forming colonies, plants growing in patches, or animals living in local communities. The population size is constrained by the limited amount of resources available in the local environment. Nevertheless, a species may expand by spreading to multiple locations and forming many local populations. In such circumstances, the

success of a species should be measured by its *overall* abundance in the long term.

The birth-death processes of a population have been studied using statistical physics models [4]. We generalize such models to include multiple local populations and migration between them. The generalized model is used to study the consequence of demographic fluctuations on the expansion of a species’ overall abundance. We find a trade-off between phenotypes that offer either a fast growth rate or a low extinction risk for the local population. A diversifying strategy that generates coexisting subpopulations of both phenotypes may yield the maximum expansion rate for the species. Generalizing our model to include local environmental variations that occur independently for different patches, we show that bet-hedging can be a universal defense mechanism against both spatio-temporal environmental variations and demographic fluctuations.

Consider an asexual organism that live in a constant environment consisting of L separate “patches”. Each patch can be either empty or occupied by a finite number of individuals. For simplicity, we assume that all patches have the same carrying capacity K , and individuals may migrate between any pair of patches (corresponding to the “structured metapopulation model” [5]). The population dynamics is modeled by three stochastic processes: birth and death within local patches, and migration between patches. Denote an individual in a patch i by \mathbb{I}_i and a vacant space by \emptyset_i , where $i = 1, \dots, L$. Then the birth, death processes within a patch i and the migration process between two patches i and j are described by:

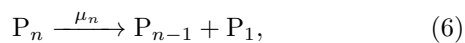


It follows that the local population size cannot exceed the carrying capacity, and that a fully occupied patch

is stable (Appendix A 1)¹. The rate constants in (1-3) are scaled such that, under mass-action kinetics, the birth and death rates per capita are given by β and δ when the local population size is small ($\ll K$), and the migration rate per capita is μ when the overall occupancy of the patches is low ($\ll L$). In this model, we assume that migration is carried out passively by external forces that determine the migration rate μ , and only consider the birth and death rates (β, δ) as individual traits of a species².

Consider first a local population in the absence of migration, described by the processes (1, 2). The deterministic dynamics of the population size n , treated as a continuous variable, is given by the logistic growth, $\dot{n} = r n(1 - n/K)$, with a maximum per capita growth rate $r = \beta - \delta$. Demographic fluctuations are stochastic variations around the deterministic dynamics, taking into account the discreteness of n . As a consequence, a local population has a nonzero probability of going extinct within a finite time. In particular, for $K \gg 1$, the extinction probability of a new population founded by one individual is given by $q = \delta/\beta$ (Appendix A 1). We assume $\beta > \delta > 0$, so that $r > 0$ and $1 > q > 0$.

When migration between patches is taken into account, a species may gain overall abundance by both growing larger colonies and colonizing more patches. We will measure the evolutionary success of a species by the *asymptotic expansion rate* of its overall abundance in the long term. This can be calculated by considering the following ‘‘patch dynamics’’³. Since all patches are equal in growth conditions and dispersal connectivity, two patches are indistinguishable if they have the same local population size n . Therefore, patches can be classified into types $\{P_n\}$, where $n = 0, \dots, K$. Let m_n be the number of each type of patches, then the number of all occupied patches is $M = \sum_{n=1}^K m_n$, and the total population size of the species is $N = \sum_{n=1}^K n m_n$. In the limit of a large number of available patches, $L \rightarrow \infty$, the birth, death, and migration processes corresponding to Eqs. (1-3) can be equivalently described by:



where the rate constants β_n , δ_n , and μ_n are $\beta_n = \beta n(1 - n/K)$, $\delta_n = \delta n(1 - n/K)$, and $\mu_n = \mu n$. To

find the asymptotic expansion rate of the species, it suffices to consider the deterministic dynamics of the patch numbers, given by

$$\begin{aligned} \dot{m}_n = & \beta_{n-1} m_{n-1} + (\delta_{n+1} + \mu_{n+1}) m_{n+1} \\ & - (\beta_n + \delta_n + \mu_n) m_n + \delta_{n,1} \sum_{n'=1}^K \mu_{n'} m_{n'}, \end{aligned} \quad (7)$$

for $n = 1, \dots, K$, where $m_{K+1} \equiv 0$. This can be written as $\dot{\mathbf{m}} = \mathbf{H} \cdot \mathbf{m}$ for the vector $\mathbf{m} \equiv (m_1, \dots, m_K)^T$, where \mathbf{H} is a constant matrix (Appendix B 1). The largest (real) eigenvalue of \mathbf{H} gives the asymptotic expansion rate, W , and the corresponding (right) eigenvector gives the steady distribution of the patch numbers.

Analytic expressions of W can be obtained in the limit where μ is large or small (Appendix B 1). For $\mu \gg \beta, \delta$, one finds $W \approx r$. Intuitively, when the migration rate is high, individuals move freely between patches, so that the whole species behaves as one population with an unlimited capacity; hence the asymptotic expansion rate is given by the growth rate r . On the other hand, for $\mu \ll \beta/K, \delta/K$, one finds $W \approx \mu K(1 - q)$. Intuitively, when the migration rate is low, the occupied patches are mostly full, hence the overall rate of migration to new patches is proportional to μK ; among those colonization attempts, only a fraction escapes local extinction, hence the factor $(1 - q)$. Note that the value of W in the latter case is much smaller than in the former case.

Therefore, a phenotype that offers the fastest population growth rate r is evolutionarily most successful when the migration rate μ is large, whereas a phenotype that yields the lowest chance of local extinction q is most favorable when μ is small. One may draw an analogy to the case of a single population in a temporally varying environment, which exhibits a trade-off between phenotypes that are favorable for different environmental conditions. In that case, a mixed strategy (‘‘bet-hedging’’) that produces coexisting individuals of different phenotypes may be more favorable than any pure strategy where all individuals have a same phenotype [3]. In the present case, could a mixed strategy between a ‘‘fast-growing’’ phenotype and a ‘‘better-surviving’’ phenotype be favorable?

Consider, for simplicity, two phenotypes A and B, which have birth and death rates (β_A, δ_A) and (β_B, δ_B) respectively. Assume that they satisfy $r_A > r_B$ and $q_A > q_B$, hence phenotype A is fast-growing and phenotype B is better-surviving. When an individual is born, it may randomly express one of the phenotypes with probabilities $\pi_A = \rho$ and $\pi_B = 1 - \rho$ respectively ($0 \leq \rho \leq 1$), regardless of the parental phenotype⁴. Let \mathbb{I}^a denote an individual of phenotype $a = A$ or B, then the birth,

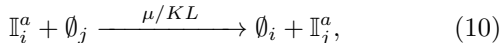
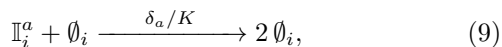
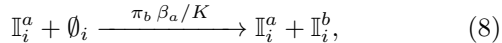
¹ Some metapopulation models assume a fixed rate of extinction (or ‘‘catastrophe’’) for every local population (e.g., [5–7]). This will effectively subtract a constant from the asymptotic expansion rate calculated below, which will not change the relative optimality of different evolutionary strategies in our model.

² For models that also optimize over dispersal rates, see, e.g., [8].

³ Similar methods are used in treating structured metapopulation models, see, e.g., [7].

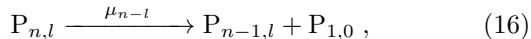
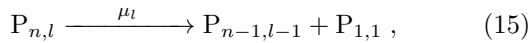
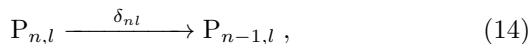
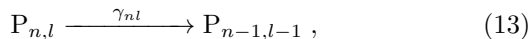
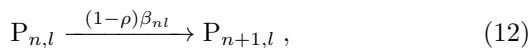
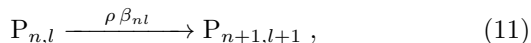
⁴ A more general case with parent-dependent phenotypic switching probabilities is discussed in Appendix E. The results are qualitatively the same as in the simple case considered here.

death, and migration processes are described by:



Note that the migration rate is assumed to not depend on the individual phenotype.

To calculate the asymptotic expansion rate of the species, we proceed as before by deriving the patch dynamics from the individual dynamics. In this case, patches can be classified by their types P_{nl} , where n is the local population size, and l is the number of individuals with phenotype A (so the number of phenotype B is $n - l$), satisfying $0 \leq n \leq K$ and $0 \leq l \leq n$. For an unlimited number of available patches, $L \rightarrow \infty$, the patch dynamics can be described by the stochastic processes:



where the rate constants are $\beta_{nl} = (\beta_A l + \beta_B (n-l)) (1 - n/K)$, $\gamma_{nl} = \delta_A l (1 - n/K)$, and $\delta_{nl} = \delta_B (n-l) (1 - n/K)$. The deterministic dynamics of the patch numbers $\{m_{nl}\}$ is again given by a set of linear dynamical equations, and the asymptotic expansion rate W is given by the largest eigenvalue of the associated matrix (Appendix B 2).

Importantly, W now depends on the phenotype distribution ρ . Let ρ^* be the value of ρ that maximizes W . If $\rho^* = 1$ or 0, then a pure strategy with a single phenotype A or B is evolutionarily most successful. However, if the maximum W is reached at an intermediate value $0 < \rho^* < 1$, then a mixed strategy in which a species constantly diversify into subpopulations of both phenotypes will be more successful in the long term.

The optimal phenotype distribution ρ^* depends on the migration rate μ . In the limit of large μ , the maximum W is achieved at $\rho^* = 1$, because in this limit, as for the single phenotype case, W is determined by the growth rate of local populations; the higher the percentage of phenotype A is, the faster the population grows. On the other hand, in the limit of small μ , one may expect $\rho^* = 0$, because W is limited by the survival chance of newly founded colonies; the larger the proportion of individuals with phenotype B, the lower the extinction risk. Those expectations are borne out by perturbative calculations similar to those for a single phenotype (Appendix B 2). Fig. 1 shows a typical example of ρ^* plotted as a function of μ (Appendix C). There is a critical value μ_L below which $\rho^* = 0$, and another critical value μ_R above which

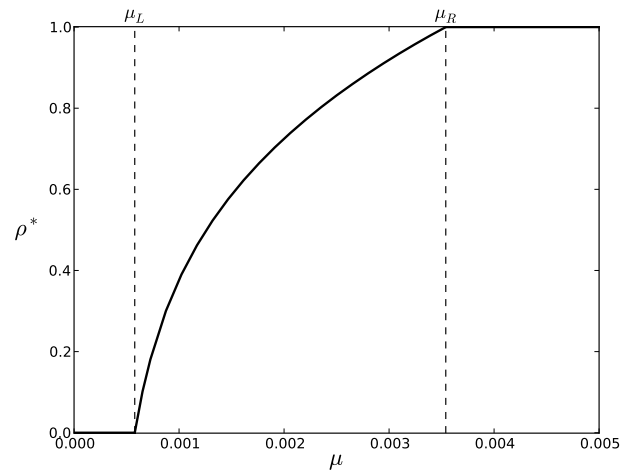


FIG. 1. Optimal phenotype distribution ρ^* as a function of migration rate μ , where one phenotype has a faster growth rate and the other has a lower extinction risk. The birth and death rates of each phenotype are $\beta_A = 2$, $\delta_A = 1$, and $\beta_B = 0.5$, $\delta_B = 0.1$; the carrying capacity of each local patch is $K = 100$. For migration rates between μ_L and μ_R , a mixed strategy offers the maximum asymptotic expansion rate for the species.

$\rho^* = 1$. In between those values, ρ^* increases continuously and monotonically from 0 to 1. Therefore, for $\mu_L < \mu < \mu_R$, a mixed strategy with $0 < \rho^* < 1$ is more favorable for maximizing the long term abundance of the species. The existence of such a favorable mixed strategy supports the idea that phenotypic diversification can be useful against uncertainties in demographic fluctuations.

Our model can be generalized to include temporal environmental variations that occur independently for different patches. This case is in contrast to the common setup for studying bet-hedging strategies where the environment varies uniformly for the whole (single) population⁵. For simplicity, assume that there are two possible environmental conditions, X and Y, where X is the “normal” environment considered above, and Y is a “hostile” environment such that the fast-growing phenotype A in environment X becomes unfavorable in Y, while the better-surviving phenotype B is unaffected. A particularly relevant example is bacterial populations that produce both normal cells which thrive in growth media but die under antibiotic treatment and persister cells which are slow-growing but tolerant to antibiotics [12]. Thus, the birth and death rates of the two phenotypes satisfy $\beta_A^{(X)} > \beta_A^{(Y)} = 0$, $\delta_A^{(Y)} \gg \delta_A^{(X)}$, and $\beta_B^{(Y)} = \beta_B^{(X)}$, $\delta_B^{(Y)} = \delta_B^{(X)}$. Each local patch switches randomly be-

⁵ but see [9, 10] for generalizations that include two local populations and migration between them. See also [11] for range expansion in a multi-patch environment with nonuniform growth conditions.

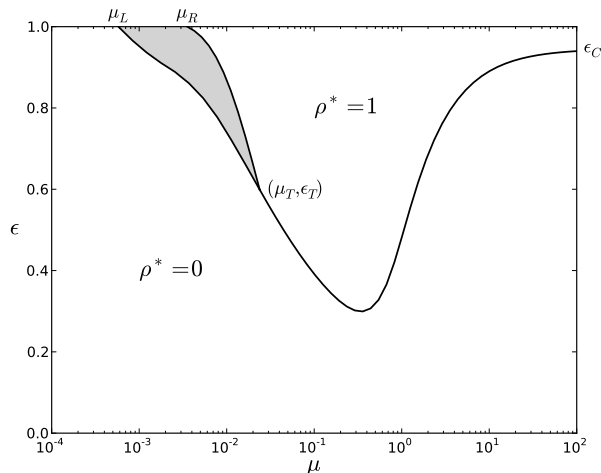


FIG. 2. Optimal phenotype distribution ρ^* for different values of the migration rate μ and the environment distribution ϵ . Shaded region marks a $0 < \rho^* < 1$ phase in which a mixed strategy offers the maximum asymptotic expansion rate. The birth and death rates of the phenotypes A, B in the environment X are the same as for Fig. 1, and that in Y are $\beta_A^{(Y)} = 0$, $\delta_A^{(Y)} = 10$, $\beta_B^{(Y)} = 0.5$, $\delta_B^{(Y)} = 0.1$. The carrying capacity of each local patch is $K = 100$, and the sum of the environmental switching rates is $\alpha_X + \alpha_Y = 0.1$.

tween the two environmental conditions, with switching rates α_X ($Y \rightarrow X$) and α_Y ($X \rightarrow Y$). The carrying capacity of each patch should be finite for both environments; for simplicity we take them to be the same, K . We also assume that the migration rate μ does not depend on the local environment. To see the effect of local environmental variations, we hold the sum of the switching rates $\alpha = \alpha_X + \alpha_Y$ fixed, and vary the fraction $\epsilon = \alpha_X/\alpha$, which measures the stationary distribution of the environment over time.

As before, the asymptotic expansion rate W of a species in this patchy and fluctuating environment can be obtained from the patch dynamics (Appendix B3). The optimal phenotype distribution ρ^* that maximizes W now depends on both the migration rate μ and the environment distribution ϵ . This can be characterized by a “phase diagram” shown in Fig. 2 (Appendix C). The topology of the phase diagram is largely determined by the behavior of ρ^* at $\epsilon = 0$ and 1, as well as the behavior in the limits $\mu \rightarrow 0$ and ∞ , which can be found analytically (Appendix B3). The top border ($\epsilon = 1$) corresponds to the case where the environment is X at all times, as shown in Fig. 1. The bottom border ($\epsilon = 0$) has $\rho^* = 0$ for all μ since it is disadvantageous to have phenotype A when the environment is Y at all times. On the far left ($\mu < \mu_L$), $\rho^* = 0$ for all ϵ because phenotype A is already disadvantageous when the environment is always favorable ($\epsilon = 1$), let alone when it is occasionally hostile ($\epsilon < 1$). On the far right ($\mu \gg \mu_R$), there is a critical value ϵ_C , above which $\rho^* = 1$ and below which $\rho^* = 0$

(Appendix B3). An asymptotically horizontal boundary, across which ρ^* undergoes a discontinuous transition, extends smoothly to smaller values of μ until reaching a point (μ_T, ϵ_T) , at which it splits into two branches. The upper branch, ending at $(\mu_R, 1)$, represents the edge of the $\rho^* = 1$ phase, whereas the lower branch, ending at $(\mu_L, 1)$, represents the edge of the $\rho^* = 0$ phase. Between these two boundaries, there exists a $0 < \rho^* < 1$ phase where a mixed strategy is optimal.

The existence of the $0 < \rho^* < 1$ phase demonstrates the usefulness of bet-hedging strategies against both demographic and environmental variations. In Appendix D we show more examples of the possible phase diagrams. In particular, an optimal bet-hedging strategy could arise mainly as a result of demographic fluctuations, such as when phenotype A is fast-growing and phenotype B is better-surviving in both environments X and Y (Fig. D1a). Alternatively, bet-hedging may be optimal mainly due to environmental variations, such as when phenotype A is both fast-growing and better-surviving in environment X, whereas phenotype B is fast-growing and better-surviving in Y (Fig. D1b). The latter case is similar to the commonly studied situation of a single population in a uniformly varying environment (Appendix D1).

Our result shows the generality of bet-hedging as a means of dealing with demographic as well as environmental variations encountered by growing populations. In our model, we have assumed that migration is instantaneous and of infinite range (i.e., patches are fully connected). One could consider cases where the patches are spatially ordered and the range of dispersal is limited (e.g., “spatially explicit” metapopulation models [5]). Furthermore, if migration takes a significant amount of time, then there may be a pool of individuals which have emigrated from but yet to immigrate into different patches (e.g., [6, 7]). These scenarios can be accommodated in our model by modifying the migration processes in the patch dynamics, yet the topology of the phase diagram and the optimality of the bet-hedging strategy are expected to be preserved. In reality, organisms live in much more complex environments — for instance, different patches may have different growth rates and carrying capacities, which would further complicate the analysis. Nevertheless, our simple model already suggests a new and broader perspective for understanding the advantage of bet-hedging behavior widely observed in nature.

ACKNOWLEDGMENTS

We thank Edo Kussell and Luca Peliti for extremely helpful discussions and comments. This research has been partly supported by grants from the Simons Foundation to S.L. through Rockefeller University (Grant No. 345430) and Institute for Advanced Study (Grant No. 345801). B.X. is funded by Eric and Wendy Schmidt Membership in Biology at Institute for Advanced Study.

-
- [1] A. M. Simons, Proc. R. Soc. B **278**, 1601 (2011).
 - [2] A. J. Grimbergen, J. Siebring, A. Solopova, and O. P. Kuipers, Curr. Opin. Microbiol. **25**, 67 (2015).
 - [3] O. Rivoire and S. Leibler, J. Stat. Phys. **142**, 1124 (2011).
 - [4] P. L. Krapisky, S. Redner, and E. Ben-Naim, *A Kinetic View of Statistical Physics* (Cambridge University Press, 2010).
 - [5] I. Hanski, *Metapopulation Ecology* (Oxford University Press, 1999).
 - [6] O. Ronce and I. Olivieri, Am. Nat. **150**, 220 (1997).
 - [7] J. A. Metz and M. Gyllenberg, Proc. R. Soc. B **268**, 499 (2001).
 - [8] P. H. Crowley and D. Nicholas McLetchie, Am. Nat. **159**, 190 (2002).
 - [9] E. Rajon, S. Venner, and F. Menu, J. Evol. Biol. **22**, 2094 (2009).
 - [10] O. Carja, R. E. Furrow, and M. W. Feldman, Proc. R. Soc. B **281**, 20141677 (2014).
 - [11] P. Patra and S. Klumpp, Phys. Rev. E **89**, 030702 (2014).
 - [12] N. Q. Balaban, J. Merrin, R. Chait, L. Kowalik, and S. Leibler, Science **305**, 1622 (2004).
 - [13] I. Lohmar and B. Meerson, Phys. Rev. E **84**, 051901 (2011).
 - [14] B. Houchmandzadeh and M. Vallade, Phys. Rev. E **82**, 051913 (2010).

Appendix A: Probability of extinction for the birth-death processes

Here we derive the probability of extinction for a local population of individuals that undergo stochastic birth and death processes. We first treat the case of a single phenotype, and then generalize to the case of a mixed strategy with two phenotypes.

1. single phenotype

For a single phenotype, the birth and death processes are described by (see Eqs. (1,2) in the main text)



where \mathbb{I} represents an individual and \emptyset represents a vacancy in a local patch with carrying capacity K . Note that Eq. (A1) means an individual has to find a vacancy within the patch in order to reproduce, which ensures that the local population size does not exceed the carrying capacity. Eq. (A2) is analogous to a continuous time Moran process — an individual dies by being replaced by a vacancy, which ensures that a fully occupied patch is stable.

This last assumption simplifies the analysis while keeping the main features of the birth-death processes. Indeed, compare that to an alternative death process described by $\mathbb{I} \xrightarrow{\delta} \emptyset$, where the death rate per capita does not depend on the population size. The latter process, together with Eq. (A1), would lead to a deterministic dynamics of the population size given by $\dot{n} = \beta n(1-n/K) - \delta n$. This is equivalent to $\dot{n} = r n(1-n/\tilde{K})$, where $r = \beta - \delta$ as before, and $\tilde{K} = Kr/\delta$ is the effective carrying capacity. Therefore, at the level of deterministic dynamics, the latter death process simply amounts to redefining the carrying capacity K . On the stochastic level, however, the latter process allows the population size to fluctuate even after reaching the carrying capacity, which results in a nonzero rate of extinction due to large fluctuations [13]. Nevertheless, this rate of extinction is exponentially small in K , which is well beyond the timescale of local extinction during range expansion considered in this paper (see below). Therefore, we may safely neglect such instability of a fully occupied patch, which justifies our choice of Eq. (A2).

Let $\mathbb{P}_n(t)$ be the probability that the population size is n at time t , where $0 \leq n \leq K$. Then $\mathbb{P}_n(t)$ obeys the master equation:

$$\begin{aligned} \frac{d\mathbb{P}_n}{dt} = & \beta(n-1)(1-(n-1)/K)\mathbb{P}_{n-1} \\ & + \delta(n+1)(1-(n+1)/K)\mathbb{P}_{n+1} \\ & - (\beta + \delta)n(1-n/K)\mathbb{P}_n. \end{aligned} \quad (\text{A3})$$

This equation can be solved by using the generating function [14]

$$\Phi(z, t) \equiv \sum_{n=0}^K \mathbb{P}_n(t) z^n, \quad (\text{A4})$$

which obeys the equation

$$\frac{\partial \Phi}{\partial t} = (1-z)(\delta - \beta z) \frac{\partial}{\partial z} \left(\Phi - \frac{z}{K} \frac{\partial \Phi}{\partial z} \right). \quad (\text{A5})$$

It can be seen that $\frac{\partial \Phi}{\partial t} = 0$ for $z = 1$ and $z = q \equiv \delta/\beta$, hence

$$\Phi(1, t) = \text{const} = 1, \quad (\text{A6})$$

$$\Phi(q, t) = \text{const} = \Phi(q, 0), \quad (\text{A7})$$

for all $t \geq 0$.

Suppose initially there are n_0 individuals, so that $\Phi(z, 0)$ is given by

$$\Phi(z, 0) = z^{n_0}. \quad (\text{A8})$$

For a finite K , the population size will eventually reach a stationary distribution, determined by the generating function $\Phi_s(z)$ satisfying

$$\frac{d}{dz} \left(\Phi_s - \frac{z}{K} \frac{d\Phi_s}{dz} \right) = 0. \quad (\text{A9})$$

The general solution is $\Phi_s(z) = C_1 + C_2 z^K$, which means the population either goes extinct or reaches full capacity. The constants C_1 and C_2 can be fixed by using boundary conditions (A6, A7), yielding

$$\Phi_s(z) = \frac{q^{n_0} - q^K}{1 - q^K} + \frac{1 - q^{n_0}}{1 - q^K} z^K. \quad (\text{A10})$$

Finally, the extinction probability is given by

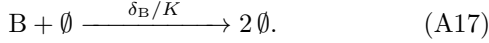
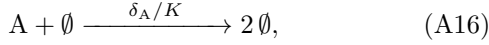
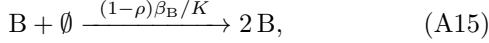
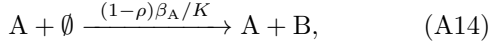
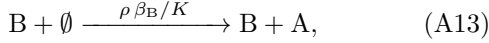
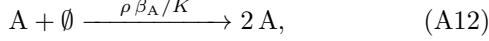
$$\begin{aligned} Q = \mathbb{P}_0(t \rightarrow \infty) &= \Phi(0, t \rightarrow \infty) = \Phi_s(0) \\ &= \frac{q^{n_0} - q^K}{1 - q^K} \approx q^{n_0}, \quad \text{for } K \gg 1. \end{aligned} \quad (\text{A11})$$

Note that the generating function $\Phi(z, t)$ converges to $\Phi_s(z)$ almost exponentially over a timescale $\sim 1/(\beta - \delta)$, hence extinction happens most likely within a short finite time.

2. mixed strategy

Now consider the case of a mixed strategy with two phenotypes $\{A, B\}$, and a constant phenotype distribution ρ . Then the birth and death processes are described

by (see Eqs. (8,9) in the main text)



Let $\mathbb{P}_{m,n}(t)$ be the probability that there are m individuals of phenotype A and n individuals of phenotype B at time t , where $0 \leq m, n \leq K$ and $0 \leq m+n \leq K$. Similarly to the single phenotype case, we define a generating function

$$\Phi(x, y, t) \equiv \sum_{m=0}^K \sum_{n=0}^{K-m} \mathbb{P}_{m,n}(t) x^m y^n, \quad (\text{A18})$$

which obeys the equation

$$\begin{aligned} \frac{\partial \Phi}{\partial t} = & \left[\left((1-x)(\delta_A - \rho\beta_A x) - (1-y)(1-\rho)\beta_A x \right) \frac{\partial}{\partial x} \right. \\ & \left. + \left((1-y)(\delta_B - (1-\rho)\beta_B y) - (1-x)\rho\beta_B y \right) \frac{\partial}{\partial y} \right] \\ & \left(\Phi - \frac{x}{K} \frac{\partial \Phi}{\partial x} - \frac{y}{K} \frac{\partial \Phi}{\partial y} \right). \end{aligned} \quad (\text{A19})$$

There are three fixed points where $\frac{\partial \Phi}{\partial t} = 0$, given by the set of equations

$$\begin{cases} (1-x)(\delta_A - \rho\beta_A x) - (1-y)(1-\rho)\beta_A x = 0, \\ (1-x)\rho\beta_B y - (1-y)(\delta_B - (1-\rho)\beta_B y) = 0. \end{cases} \quad (\text{A20})$$

Besides the trivial solution $(x, y) = (1, 1)$ which implies normalization $\Phi(1, 1, t) = 1$, the other two are

$$\begin{cases} x_s = \frac{2q_A}{(1+q_A-q_B) + \sqrt{(1-q_A+q_B)^2 + 4(1-\rho)(q_A-q_B)}}, \\ y_s = \frac{2q_B}{(1-q_A+q_B) + \sqrt{(1-q_A+q_B)^2 + 4(1-\rho)(q_A-q_B)}}; \end{cases} \quad (\text{A21})$$

$$\begin{cases} x_1 = \frac{(1+q_A-q_B) + \sqrt{(1-q_A+q_B)^2 + 4(1-\rho)(q_A-q_B)}}{2\rho(q_A-q_B)/q_A}, \\ y_1 = \frac{(1-q_A+q_B) + \sqrt{(1-q_A+q_B)^2 + 4(1-\rho)(q_A-q_B)}}{2(1-\rho)(q_A-q_B)/q_B}, \end{cases} \quad (\text{A22})$$

where $q_A \equiv \delta_A/\beta_A$ and $q_B \equiv \delta_B/\beta_B$. It follows that

$$\Phi(x_s, y_s, t) = \Phi(x_s, y_s, 0) = x_s^{m_0} y_s^{n_0}, \quad (\text{A23})$$

and similarly for (x_1, y_1) , where m_0, n_0 are the initial numbers of individuals with phenotype A and B respectively. Note that $0 < x_s, y_s < 1 < x_1, y_1$, which will be useful later.

Since the population will eventually either go extinct or reach full capacity, the generating function $\Phi_s(x, y)$ that

corresponds to the stationary distribution $\mathbb{P}_{m,n}(t \rightarrow \infty)$ should be of the form

$$\Phi_s(x, y) = Q + (1-Q) \sum_{\ell=0}^K C_\ell x^\ell y^{K-\ell}, \quad (\text{A24})$$

where the constants $\{C_\ell\}$ satisfy $\sum_{\ell=0}^K C_\ell = 1$, and Q is the extinction probability, $Q = \Phi_s(0, 0) = \mathbb{P}_{0,0}(t \rightarrow \infty)$. We have already used the normalization condition $\Phi_s(1, 1) = 1$. Since there are not enough conserved quantities like Eq. (A23), we cannot fix all constants $\{C_\ell\}$ without actually solving the equation (A19) from initial conditions. However, an approximation of Q can be obtained by using Eq. (A23), which gives

$$\Phi_s(x_s, y_s) = Q + (1-Q) \sum_{\ell=0}^K C_\ell x_s^\ell y_s^{K-\ell} = x_s^{m_0} y_s^{n_0}. \quad (\text{A25})$$

Notice that all terms involving $\{C_\ell\}$ are K -th order in x_s and y_s , while the last term is of order $m_0 + n_0$; since $0 < x_s, y_s < 1$, for $K \gg m_0 + n_0 \geq 1$ we obtain

$$Q \approx x_s^{m_0} y_s^{n_0}. \quad (\text{A26})$$

In particular, $Q \approx x_s$ if $(m_0, n_0) = (1, 0)$, and y_s if $(m_0, n_0) = (0, 1)$.

Therefore, x_s is the extinction probability of a local population founded by an individual of phenotype A, and y_s is that for phenotype B. Note that, for $q_A > q_B$, one finds $x_s > y_s$ for all ρ , since, intuitively, phenotype A is more prone to demographic fluctuation that may cause extinction. For the same reason, both x_s and y_s increases monotonically with ρ , which is obvious from Eq. (A21). In the limit $\rho \rightarrow 1$ we have $x_s \rightarrow q_A$ as it should be, whereas $y_s \rightarrow q_B$ in the limit $\rho \rightarrow 0$.

Appendix B: Approximate expressions of the asymptotic expansion rate W

Here we derive the asymptotic expansion rate W in the limit of small and large migration rate μ . We first illustrate the method by treating the simple case of a single phenotype, and then generalize to the case of a mixed strategy and of locally fluctuating environments.

1. single phenotype

Our starting point is the deterministic equation of the patch numbers derived from the patch dynamics. For a single phenotype, this is Eq. (7) in the main text, which can be written in a matrix form as $\dot{\mathbf{m}} = \mathbf{H} \cdot \mathbf{m}$, where

$\mathbf{m} \equiv (m_1, \dots, m_K)^T$ and

$$\mathbf{H} \equiv \begin{pmatrix} -\beta_1 - \delta_1 & \delta_2 + 2\mu_2 & \mu_3 & \cdots & \mu_K \\ \beta_1 & -\beta_2 - \delta_2 - \mu_2 & \delta_3 + \mu_3 & & \\ & \ddots & \ddots & \ddots & \\ & & \ddots & \ddots & \delta_K + \mu_K \\ & & & \beta_{K-1} & -\beta_K - \delta_K - \mu_K \end{pmatrix}. \quad (\text{B1})$$

The asymptotic expansion rate, W , is given by the largest (real) eigenvalue $\lambda^{(1)}$ of the matrix \mathbf{H} , and the steady patch number distribution is given by the corresponding (right) eigenvector $\boldsymbol{\xi}^{(1)}$, normalized such that $\sum_{n=1}^K \xi_n^{(1)} = 1$.

Analytic expressions of W can be obtained in the limits where the migration rate μ is large or small. Notice that the matrix \mathbf{H} can be separated into two parts, one independent of μ and the other proportional to μ ,

$$\mathbf{H} = \begin{pmatrix} -\beta_1 - \delta_1 & \delta_2 & & & \\ \beta_1 & -\beta_2 - \delta_2 & \delta_3 & & \\ & \ddots & \ddots & \ddots & \\ & & \ddots & \ddots & \delta_K \\ & & & \beta_{K-1} & -\beta_K - \delta_K \end{pmatrix} + \begin{pmatrix} 0 & 2\mu_2 & \mu_3 & \cdots & \mu_K \\ -\mu_2 & \mu_3 & & & \\ & \ddots & \ddots & & \\ & & \ddots & \mu_K & \\ & & & -\mu_K & \end{pmatrix} \equiv \mathbf{H}^{\beta\delta} + \mathbf{H}^\mu. \quad (\text{B2})$$

When $\mu \gg \beta, \delta$, one can treat \mathbf{H}^μ as the dominant part and $\mathbf{H}^{\beta\delta}$ as a perturbation. The largest eigenvalue of \mathbf{H}^μ is $\lambda^\mu = 0$, and its right and left eigenvectors are $\boldsymbol{\xi}^\mu = (1, 0, \dots, 0)^T$ and $\boldsymbol{\eta}^\mu = (1, 2, \dots, K)^T$. The first-order perturbation of the eigenvalue is given by

$$\Delta\lambda^{(1)} = \boldsymbol{\eta}^{\mu T} \cdot \mathbf{H}^{\beta\delta} \cdot \boldsymbol{\xi}^\mu = (\beta - \delta)(1 - 1/K). \quad (\text{B3})$$

Therefore, assuming $K \gg 1$, the asymptotic expansion rate is approximately given by

$$W \approx r. \quad (\text{B4})$$

When $\mu \ll \beta/K, \delta/K$, one can instead treat $\mathbf{H}^{\beta\delta}$ as the dominant part and \mathbf{H}^μ as a perturbation. Since $\beta_K = \delta_K = 0$, the largest eigenvalue of $\mathbf{H}^{\beta\delta}$ is also zero, $\lambda^{\beta\delta} = 0$, and its eigenvectors are $\boldsymbol{\xi}^{\beta\delta} = (0, \dots, 0, 1)^T$ and $\boldsymbol{\eta}^{\beta\delta} = \{(1 - q^n)/(1 - q^K), n = 1, \dots, K\}$. Hence the first-order perturbation of the eigenvalue is

$$\Delta\lambda^{(1)} = \boldsymbol{\eta}^{\beta\delta T} \cdot \mathbf{H}^\mu \cdot \boldsymbol{\xi}^{\beta\delta} = \mu K(1 - q) \frac{(1 - q^{K-1})}{(1 - q^K)}. \quad (\text{B5})$$

Therefore, assuming $K \gg 1$, one finds

$$W \approx \mu K(1 - q). \quad (\text{B6})$$

2. mixed strategy

For a mixed strategy, the deterministic equation of the patch numbers corresponding to the patch dynamics (11-16) in the main text is

$$\begin{aligned} \dot{m}_{n,l} &= \rho \beta_{n-1,l-1} m_{n-1,l-1} + (1 - \rho) \beta_{n-1,l} m_{n-1,l} \\ &+ (\gamma_{n+1,l+1} + \mu_{l+1}) m_{n+1,l+1} + (\delta_{n+1,l} + \mu_{n-l+1}) m_{n+1,l} \\ &- (\beta_{n,l} + \gamma_{n,l} + \delta_{n,l} + \mu_n) m_{n,l} \\ &+ \delta_{n,1} \sum_{n'=1}^K \sum_{l'=0}^{n'} (\delta_{l,1} \mu_{l'} + \delta_{l,0} \mu_{n'-l'}) m_{n',l'}, \end{aligned} \quad (\text{B7})$$

where $n = 1, \dots, K$ and $l = 0, \dots, n$; the rate constants are $\beta_{nl} = (\beta_A l + \beta_B(n-l))(1 - n/K)$, $\gamma_{nl} = \delta_A l(1 - n/K)$, and $\delta_{nl} = \delta_B(n-l)(1 - n/K)$. Note that $m_{n,l}$ is set to 0 for $n = 0, K+1$ and for $l < 0$ or $l > n$. This equation can also be cast in a matrix form for a vector \mathbf{m} with composite indices (nl) , i.e., $\dot{m}_{nl} = \sum_{n'l'} \mathbf{H}_{nl,n'l'} m_{n'l'}$. The elements of the matrix \mathbf{H} are

$$\begin{aligned} \mathbf{H}_{nl,n'l'} &= \rho \beta_{n',l'} \delta_{n',n-1} \delta_{l',l-1} + (1 - \rho) \beta_{n',l'} \delta_{n',n-1} \delta_{l',l} \\ &+ (\gamma_{n',l'} + \mu_{l'}) \delta_{n',n+1} \delta_{l',l+1} + (\delta_{n',l'} + \mu_{n'-l'}) \delta_{n',n+1} \delta_{l',l} \\ &- (\beta_{n',l'} + \gamma_{n',l'} + \delta_{n',l'} + \mu_{n'}) \delta_{n',n} \delta_{l',l} \\ &+ \delta_{n,1} (\delta_{l,1} \mu_{l'} + \delta_{l,0} \mu_{n'-l'}). \end{aligned} \quad (\text{B8})$$

The asymptotic expansion rate W is given by the largest (real) eigenvalue of this matrix \mathbf{H} .

Like for Eq. (B2), \mathbf{H} can be decomposed as $\mathbf{H} = \mathbf{H}^{\beta\delta} + \mathbf{H}^\mu$, where

$$\begin{aligned} \mathbf{H}_{nl,n'l'}^{\beta\delta} &= \rho \beta_{n',l'} \delta_{n',n-1} \delta_{l',l-1} + (1 - \rho) \beta_{n',l'} \delta_{n',n-1} \delta_{l',l} \\ &+ \gamma_{n',l'} \delta_{n',n+1} \delta_{l',l+1} + \delta_{n',l'} \delta_{n',n+1} \delta_{l',l} \\ &- (\beta_{n',l'} + \gamma_{n',l'} + \delta_{n',l'}) \delta_{n',n} \delta_{l',l}, \end{aligned} \quad (\text{B9})$$

$$\begin{aligned} \mathbf{H}_{nl,n'l'}^\mu &= \mu_{l'} \delta_{n',n+1} \delta_{l',l+1} + \mu_{n'-l'} \delta_{n',n+1} \delta_{l',l} \\ &- \mu_{n'} \delta_{n',n} \delta_{l',l} + \delta_{n,1} (\delta_{l,1} \mu_{l'} + \delta_{l,0} \mu_{n'-l'}). \end{aligned} \quad (\text{B10})$$

Thus $\mathbf{H}^{\beta\delta}$ is independent of μ , and \mathbf{H}^μ is proportional to μ . In the limit of large or small μ , the leading eigenvalue of \mathbf{H} can be calculated using perturbative methods as before.

For large μ , we again treat \mathbf{H}^μ as the dominant part and $\mathbf{H}^{\beta\delta}$ as a perturbation. The largest eigenvalue of \mathbf{H}^μ is 0, which turns out to be degenerate with degree 2. The right eigenvectors corresponding to this eigenvalue are $\boldsymbol{\xi}_{nl}^{(1)} = \delta_{n,1} \delta_{l,1}$ and $\boldsymbol{\xi}_{nl}^{(2)} = \delta_{n,1} \delta_{l,0}$. Since the leading eigenvector of \mathbf{H} represents the steady patch number distribution, it means that the leading contribution to the steady distribution comes from patches that are occupied by just one individual, $n = 1$. This agrees with our intuition that, in the limit of frequent migration, individuals are scattered out over many patches.

The left eigenvectors that are orthonormal to $\boldsymbol{\xi}^{(1)}$ and $\boldsymbol{\xi}^{(2)}$ are $\boldsymbol{\eta}_{nl}^{(1)} = l$ and $\boldsymbol{\eta}_{nl}^{(2)} = n - l$. Therefore, the first-order perturbation of the degenerate eigenvalues are

given by the 2×2 matrix

$$\begin{aligned} \Delta \mathbf{H}^\mu &= \begin{pmatrix} \boldsymbol{\eta}^{(1)T} \\ \boldsymbol{\eta}^{(2)T} \end{pmatrix} \cdot \mathbf{H}^{\beta\delta} \cdot (\boldsymbol{\xi}^{(1)} \quad \boldsymbol{\xi}^{(2)}) \quad (\text{B11}) \\ &= \left(1 - \frac{1}{K}\right) \begin{pmatrix} \rho\beta_A - \delta_A, & \rho\beta_B \\ (1-\rho)\beta_A, & (1-\rho)\beta_B - \delta_B \end{pmatrix}. \end{aligned}$$

It may be recognized that, for $K \rightarrow \infty$, this is exactly the growth matrix that governs the deterministic dynamics of a single mixed population (see Eqs. (A12-A17)),

$$\dot{n}_A = (\rho\beta_A - \delta_A)n_A + \rho\beta_B n_B, \quad (\text{B12})$$

$$\dot{n}_B = (1-\rho)\beta_A n_A + ((1-\rho)\beta_B - \delta_B)n_B. \quad (\text{B13})$$

The growth rate of this mixed population is given by the larger eigenvalue of the growth matrix,

$$\begin{aligned} r_m(\rho) &= \frac{1}{2} \left[(\rho\beta_A - \delta_A + (1-\rho)\beta_B - \delta_B) \quad (\text{B14}) \right. \\ &\quad \left. + \sqrt{(\rho\beta_A - \delta_A - (1-\rho)\beta_B + \delta_B)^2 + 4\rho(1-\rho)\beta_A\beta_B} \right]. \end{aligned}$$

Therefore, we recover the relation $W \approx r_m(\rho)$, as in Eq. (B4).

One can easily check that $r_m(0) = r_B$ and $r_m(1) = r_A$, where $r_a \equiv \beta_a - \delta_a$ for each phenotype $a = A, B$. For $0 < \rho < 1$, the value of $r_m(\rho)$ lies in between r_B and r_A . Indeed, for $r_A > r_B$, one finds that $r_m(\rho)$ increases monotonically with ρ , since

$$\begin{aligned} r'_m(\rho) &= \frac{(r_A - r_B)r_m + (r_m - r_B)\delta_A + (r_A - r_m)\delta_B}{\sqrt{(\rho\beta_A - \delta_A - (1-\rho)\beta_B + \delta_B)^2 + 4\rho(1-\rho)\beta_A\beta_B}} \\ &> 0. \quad (\text{B15}) \end{aligned}$$

For small μ , $\mathbf{H}^{\beta\delta}$ becomes the dominant part of \mathbf{H} , and \mathbf{H}^μ the perturbation. Since $\beta_{K,l} = \delta_{K,l} = 0$ for all $l = 0, \dots, K$, the largest eigenvalue of $\mathbf{H}^{\beta\delta}$, $\lambda^{(1)} = 0$, is $(K+1)$ -degree degenerate. The corresponding right eigenvectors are simply $\boldsymbol{\xi}_{nl}^{(s)} = \delta_{n,K}\delta_{l,s}$, where $s = 0, \dots, K$. Unfortunately, not all left eigenvectors can be found analytically (there is one, $\boldsymbol{\eta}_{nl} \propto 1 - x_s^l y_s^{n-l}$, where x_s, y_s are given in Sec. A2). Therefore, we will resort to a different method based on the following approximation.

As shown by the eigenvectors $\boldsymbol{\xi}_{nl}^{(s)}$, in the limit of rare migration, most occupied patches are full, $n = K$. Since the timescale of birth and death processes within a patch is much shorter than the migration timescale, in terms of the latter, newly occupied patches either go extinct immediately or quickly grow to full capacity. Therefore, we may ignore the partially filled patches and consider only the full patches. For $K \gg 1$, the phenotype composition of a full patch is approximately given by the eigenvector of the matrix (B11) corresponding to the eigenvalue r_m , $\boldsymbol{\xi}_m^{(1)} = (\xi_A, \xi_B)^T$, where

$$\xi_A \equiv \frac{r_m - r_B}{r_A - r_B}, \quad \xi_B \equiv \frac{r_A - r_m}{r_A - r_B}. \quad (\text{B16})$$

Therefore, for a given full patch, the rate of emigration of an individual with phenotype A is $\mu K \xi_A$, and that of an individual with phenotype B is $\mu K \xi_B$. Next we have to take into account the chance of successful colonization of a new patch by the emigrated individual. By the results from Sec. A2, the extinction probability of a local population founded by an individual of phenotype A is x_s , and that for phenotype B is y_s . Therefore, the rate of successful colonization is

$$W \approx \mu K \xi_A (1 - x_s) + \mu K \xi_B (1 - y_s) = \mu K (1 - q_m), \quad (\text{B17})$$

which has the same form as Eq. (B6), with an average extinction probability

$$q_m(\rho) \equiv \frac{r_m - r_B}{r_A - r_B} x_s + \frac{r_A - r_m}{r_A - r_B} y_s. \quad (\text{B18})$$

One readily checks that $q_m(1) = q_A$ and $q_m(0) = q_B$. For $r_A > r_B$ and $q_A > q_B$, $q_m(\rho)$ monotonically increases with ρ , since

$$q'_m(\rho) = \frac{x_s - y_s}{r_A - r_B} r'_m(\rho) + \frac{r_m - r_B}{r_A - r_B} x'_s(\rho) + \frac{r_A - r_m}{r_A - r_B} y'_s(\rho), \quad (\text{B19})$$

where each term is positive.

3. local environmental variations

We now consider the case where the local environment of each patch can switch between two conditions X and Y. Denote a patch with local environment $\varepsilon = X$ or Y by P^ε , and classify the patches by their local population size and composition as before, denoted by subscripts (nl) . Then the patch dynamics can be written as:

$$P_{n,l}^\varepsilon \xrightarrow{\rho\beta_{nl}^{(\varepsilon)}} P_{n+1,l+1}^\varepsilon, \quad (\text{B20})$$

$$P_{n,l}^\varepsilon \xrightarrow{(1-\rho)\beta_{nl}^{(\varepsilon)}} P_{n+1,l}^\varepsilon, \quad (\text{B21})$$

$$P_{n,l}^\varepsilon \xrightarrow{\gamma_{nl}^{(\varepsilon)}} P_{n-1,l-1}^\varepsilon, \quad (\text{B22})$$

$$P_{n,l}^\varepsilon \xrightarrow{\delta_{nl}^{(\varepsilon)}} P_{n-1,l}^\varepsilon, \quad (\text{B23})$$

$$P_{n,l}^\varepsilon \xrightarrow{p_{\varepsilon'} \mu_l} P_{n-1,l-1}^\varepsilon + P_{1,1}^{\varepsilon'}, \quad (\text{B24})$$

$$P_{n,l}^\varepsilon \xrightarrow{p_{\varepsilon'} \mu_{n-l}} P_{n-1,l}^\varepsilon + P_{1,0}^{\varepsilon'}, \quad (\text{B25})$$

$$P_{n,l}^X \xrightarrow{\alpha_Y} P_{n,l}^Y, \quad (\text{B26})$$

$$P_{n,l}^Y \xrightarrow{\alpha_X} P_{n,l}^X, \quad (\text{B27})$$

where the rate constants are defined similarly to that for Eqs. (11-16) except for the extra dependence on the environment. The last two equations describe the switching of local environment from Y to X and from X to Y, with rates α_X and α_Y respectively. We have again assumed an unlimited number of available patches, $L \rightarrow \infty$. A newly colonized patch will have local environment X with probability $p_X = \alpha_X / (\alpha_X + \alpha_Y) \equiv \varepsilon$, and Y with probability

$p_Y = (1 - \epsilon)$, which are used in Eqs. (B24,B25). As before, the asymptotic expansion rate W of a species in this patchy and fluctuating environment can be obtained from the deterministic dynamics of the patch numbers.

In the limit of a large migration rate μ , as argued in Sec. B 2, individuals are always scattered out over many patches. Since the local environment of each patch fluctuates randomly and independently, there is approximately a fraction ϵ of the patches having environment X and $(1 - \epsilon)$ of them having Y at any given time. Therefore, the species as a whole essentially experiences a “well mixed environment”, in which the *average* birth and death rates are

$$\bar{\beta}_a = \epsilon \beta_a^{(X)} + (1 - \epsilon) \beta_a^{(Y)}, \quad (\text{B28})$$

$$\bar{\delta}_a = \epsilon \delta_a^{(X)} + (1 - \epsilon) \delta_a^{(Y)}, \quad (\text{B29})$$

for each phenotype $a = \text{A, B}$. The problem then becomes equivalent to the case of a uniform environment treated in the previous subsection — in the limit of large μ , W is given by the growth rate r_m in Eq. (B14), calculated from the average birth and death rates above.

In this limit, the optimal phenotype distribution ρ^* can be obtained easily — whichever phenotype that yields a faster growth rate, $\bar{r}_a = \bar{\beta}_a - \bar{\delta}_a$, is evolutionarily more successful; i.e., $\rho^* = 0$ if $\bar{r}_A < \bar{r}_B$, and 1 if $\bar{r}_A > \bar{r}_B$. In the example used for Fig. 2 in the main text, we have $\bar{r}_A = \epsilon r_A - (1 - \epsilon) s_A$ and $\bar{r}_B = r_B$, where $r_A = \beta_A^{(X)} - \delta_A^{(X)}$, $s_A = \delta_A^{(Y)} - \beta_A^{(Y)}$, and $r_B = \beta_B^{(X)} - \delta_B^{(X)}$. Hence, there is a critical value $\epsilon_c = \frac{r_B + s_A}{r_A + s_A}$, above which $\rho^* = 1$ and below which $\rho^* = 0$, as shown in Fig. 2.

In the limit of small μ , we use an approximation similar to the one used in Sec. B 2. Consider a special case where phenotype A is both fast-growing and better-surviving in environment X, whereas phenotype B is fast-growing and better-surviving in Y, which will be discussed in Sec. D. Since most occupied patches are full in this limit, we may consider only the full patches, which can have environment $\epsilon = \text{X}$ or Y , denoted by P^ϵ . The phenotype composition of these two types of patches are approximately given by the eigenvectors of the corresponding growth matrices (Sec. D 1) — the fraction of phenotype B in a patch P^X is denoted ζ_B , and the fraction of phenotype A in a patch P^Y is ζ_A , satisfying $\zeta_a \ll 1$. We assume $K\zeta_a \gg 1$, so that both phenotypes are generally present in each full patch.

Under those conditions, the patch dynamics may be reduced to the following processes:

$$P^X \xrightarrow{\mu K(1 - \zeta_B)(1 - \tilde{q}_A)\epsilon} 2P^X, \quad (\text{B30})$$

$$P^Y \xrightarrow{\mu K\zeta_A(1 - \tilde{q}_A)\epsilon} P^Y + P^X, \quad (\text{B31})$$

$$P^X \xrightarrow{\mu K\zeta_B(1 - \tilde{q}_B)(1 - \epsilon)} P^X + P^Y, \quad (\text{B32})$$

$$P^Y \xrightarrow{\mu K(1 - \zeta_A)(1 - \tilde{q}_B)(1 - \epsilon)} 2P^Y, \quad (\text{B33})$$

$$P^X \xrightarrow{\alpha_Y} P^Y, \quad (\text{B34})$$

$$P^Y \xrightarrow{\alpha_X} P^X. \quad (\text{B35})$$

The first two equations represent processes in which an individual of phenotype A migrates to a patch of environment X and successfully establishes a colony; the chance of unsuccessful colonization (local extinction) is $\tilde{q}_A \equiv \max\{1, q_A/\rho\}$, where $q_A \equiv \delta_A^{(X)}/\beta_A^{(X)}$. Similarly, the second two equations represent an individual of phenotype B migrating to and successfully colonizing a patch of environment Y, where $\tilde{q}_B \equiv \max\{1, q_B/(1 - \rho)\}$ and $q_B \equiv \delta_B^{(Y)}/\beta_B^{(Y)}$. Migration of phenotype A to environment Y and phenotype B to environment X are assumed to have negligible success rates. The last two equations represent the switching of local environments; a colony would likely survive the switch if both phenotypes are present.

For the reduced processes, the deterministic dynamics of the patch numbers m_X and m_Y are given by

$$\dot{m}_X = \mu K(1 - \zeta_B)(1 - \tilde{q}_A)\epsilon m_X + \mu K\zeta_A(1 - \tilde{q}_A)\epsilon m_Y - \alpha_Y m_X + \alpha_X m_Y, \quad (\text{B36})$$

$$\dot{m}_Y = \mu K\zeta_B(1 - \tilde{q}_B)(1 - \epsilon) m_X + \mu K(1 - \zeta_A)(1 - \tilde{q}_B) \times (1 - \epsilon) m_Y + \alpha_Y m_X - \alpha_X m_Y. \quad (\text{B37})$$

This can be described by a growth matrix

$$\mathbf{H} = \begin{pmatrix} -\alpha_Y & \alpha_X \\ \alpha_Y & -\alpha_X \end{pmatrix} + \mu K \begin{pmatrix} (1 - \zeta_B)(1 - \tilde{q}_A)\epsilon & \zeta_A(1 - \tilde{q}_A)\epsilon \\ \zeta_B(1 - \tilde{q}_B)(1 - \epsilon) & (1 - \zeta_A)(1 - \tilde{q}_B)(1 - \epsilon) \end{pmatrix}. \quad (\text{B38})$$

For small μ , the leading eigenvalue which gives the asymptotic expansion rate W can be calculated by treating the second term as a perturbation. If we further ignore small factors involving ζ_A and ζ_B , then W is approximately given by

$$W \approx \mu K \left[\frac{\epsilon^2}{\rho} R(\rho - q_A) + \frac{(1 - \epsilon)^2}{(1 - \rho)} R(1 - \rho - q_B) \right], \quad (\text{B39})$$

where $R(x)$ is the ramp function, $R(x) = \max\{0, x\}$. Finally, the optimal phenotype distribution ρ^* can be obtained by maximizing W with respect to ρ .

For simplicity, consider the symmetric case where $q_A = q_B \equiv q$. For $q > \frac{1}{3}$, the maximum of W is reached at $\rho^* = 0$ for $\epsilon < \frac{1}{2}$, and $\rho^* = 1$ for $\epsilon > \frac{1}{2}$; hence there is no mixed strategy that is favorable. However, for $q < \frac{1}{3}$,

$$\rho^* = \begin{cases} 0, & 0 \leq \epsilon < \frac{2q}{1+q}; \\ \epsilon, & \frac{2q}{1+q} < \epsilon < \frac{1-q}{1+q}; \\ 1, & \frac{1-q}{1+q} < \epsilon \leq 1. \end{cases} \quad (\text{B40})$$

In this case, there is a range of intermediate ϵ values for which a mixed strategy is optimal, as shown in Fig. B1. Interestingly, the optimal phenotype distribution, $\rho^* = \epsilon$, being proportional to the environment distribution, is reminiscent of the “proportional betting” solution found for a single population in a uniformly fluctuating environment (with a slightly different setting, see [3]).

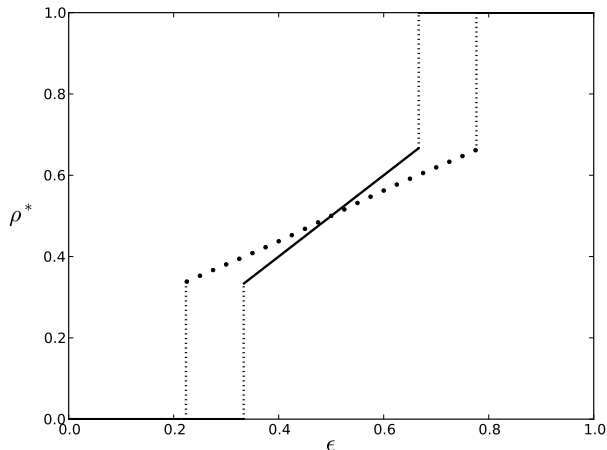


FIG. B1. Optimal phenotype distribution ρ^* with respect to the environment distribution ϵ for a small migration rate μ . The birth and death rates of each phenotype, the carrying capacity, and the sum of environmental switching rates are the same as in Fig. D1b. Continuous line is the approximate analytic result for $\mu \rightarrow 0$, according to Eq. (B40); dots are the exact results for $\mu = 10^{-4}$ obtained by numerical calculations.

Appendix C: Numerical calculation of the optimal phenotype distribution ρ^*

Here we describe how the optimal phenotype distribution ρ^* is calculated numerically, as for Figs. 1-2 in the main text.

Consider first the case of a constant environment, described in Sec. B2. For a given phenotype distribution ρ , the asymptotic expansion rate W is given by the largest real eigenvalue of the matrix \mathbf{H} in Eq. (B8). \mathbf{H} is a sparse $D \times D$ matrix, where D is the number of patch types $\{P_{nl}\}$; since $1 \leq n \leq K$ and $0 \leq l \leq n$, one finds $D = K(K+3)/2$. The eigenvalue of largest real part, W , and its left and right eigenvectors, $\boldsymbol{\eta}$ and $\boldsymbol{\xi}$, can be found by efficient numerical routines (e.g., the shift-invert method in ARPACK). It is checked that W , $\boldsymbol{\eta}$, and $\boldsymbol{\xi}$ are all real. Moreover, we may calculate the derivative of W with respect to ρ , given by

$$W'(\rho) = \boldsymbol{\eta}^\top \cdot \left(\frac{d\mathbf{H}}{d\rho} \right) \cdot \boldsymbol{\xi}, \quad (\text{C1})$$

where $\left(\frac{d\mathbf{H}}{d\rho} \right)$ is the constant matrix given by

$$\left(\frac{d\mathbf{H}}{d\rho} \right)_{nl,n'l'} = \beta_{n'l'} \delta_{n',n-1} (\delta_{l',l-1} - \delta_{l',l}). \quad (\text{C2})$$

Generalizing to the case of locally varying environments, W and $W'(\rho)$ can be numerically calculated the same way as above, except that the number of patch types, i.e., the dimension D of the matrix \mathbf{H} , is doubled to account for the two types of local environments.

Using those methods of calculating W and its derivative $W'(\rho)$, it is straight-forward to find the value of ρ^*

that maximizes W . Some examples of W as a function of ρ are shown in Figs. C1. Note that the location of ρ^* varies with the migration rate μ and the environment distribution ϵ . In the following, we describe some typical behavior of $W(\rho)$ as μ and ϵ vary, and how the location of ρ^* is obtained.

Fig. C1a shows $W(\rho)$ for different values of μ when the environment is constant, corresponding to the example shown in Fig. 1 of the main text. It can be seen that, for a small μ , the derivative $W'(\rho)$ is negative throughout $\rho = 0$ to 1, hence we have $\rho^* = 0$; for a large μ , $W'(\rho)$ is positive at all ρ , hence $\rho^* = 1$, consistent with the perturbative analysis in Sec. B2. For an intermediate value of μ for which $W'(0) > 0$ and $W'(1) < 0$, $W(\rho)$ has a local maximum at $0 < \rho^* < 1$, which is located by numerically finding the root of $W'(\rho) = 0$. In this example, we find two bounds, μ_L and μ_R , between which $0 < \rho^* < 1$. The value of μ_L is given by the condition $W'(0) = 0$, and, similarly, μ_R by $W'(1) = 0$. This procedure is used to produce Fig. 1 in the main text. Note that for some rare cases, especially when the values of r_A and r_B , or q_A and q_B , are very close, it happens that $W(\rho)$ develops a local minimum instead of a maximum (similar to Fig. C1b), signaled by $W'(0) < 0$ and $W'(1) > 0$. In such cases, ρ^* jumps discontinuously from 0 to 1 at a particular value of μ , i.e., $\mu_L = \mu_R$.

Fig. C1b shows the case of locally varying environments and how $W(\rho)$ changes with ϵ for a given μ . In particular, the parameters are the same as for Fig. 2 in the main text, and μ is fixed to a large value, $\mu > \mu_T$. It can be seen that $W(\rho)$ is monotonic decreasing ($W'(\rho) < 0$) for a small ϵ , and becomes monotonic increasing ($W'(\rho) > 0$) for a large ϵ ; for some ϵ between those values, $W(\rho)$ has a local minimum ($W'(0) < 0$ and $W'(1) > 0$). In any case, the maximum of W is reached at either $\rho^* = 0$ or 1. Therefore, it suffices to compare the values of $W(0)$ and $W(1)$ to determine ρ^* . This procedure is used to produce part of Fig. 2 for $\mu > \mu_T$, where μ_T is determined below. Note that ρ^* transitions from 0 to 1 discontinuously at a critical value ϵ_C , as shown in Fig. C1d, which is consistent with the perturbative analysis described in Sec. B3 for a large μ .

A more intricate situation is shown in Fig. C1c, where $W(\rho)$ can have multiple local maxima, one at an end of the unit interval and one in the middle. This happens for certain μ values between μ_L and μ_T in Fig. 2 — as ϵ increases from 0 to 1, a local maximum emerges at an intermediate value of ρ , even though $W'(0)$ and $W'(1)$ have the same sign. In such situations, the numerical search for ρ^* is carried out as follows. In the example shown in Fig. C1c, when both $W'(0) < 0$ and $W'(1) < 0$, the value of $W(0)$ is noted. Then one randomly searches for a value ρ_0 where $W'(\rho_0) > 0$; if such a ρ_0 is found, then one locates the local maximum ρ_1^* within the range $\rho_0 < \rho_1^* < 1$ by finding the root of $W'(\rho) = 0$. Finally, a comparison of $W(0)$ and $W(\rho_1^*)$ picks out the larger one and hence the true ρ^* . Such a procedure is used to produce part of Fig. 2 for $\mu_L < \mu < \mu_T$. Note that,

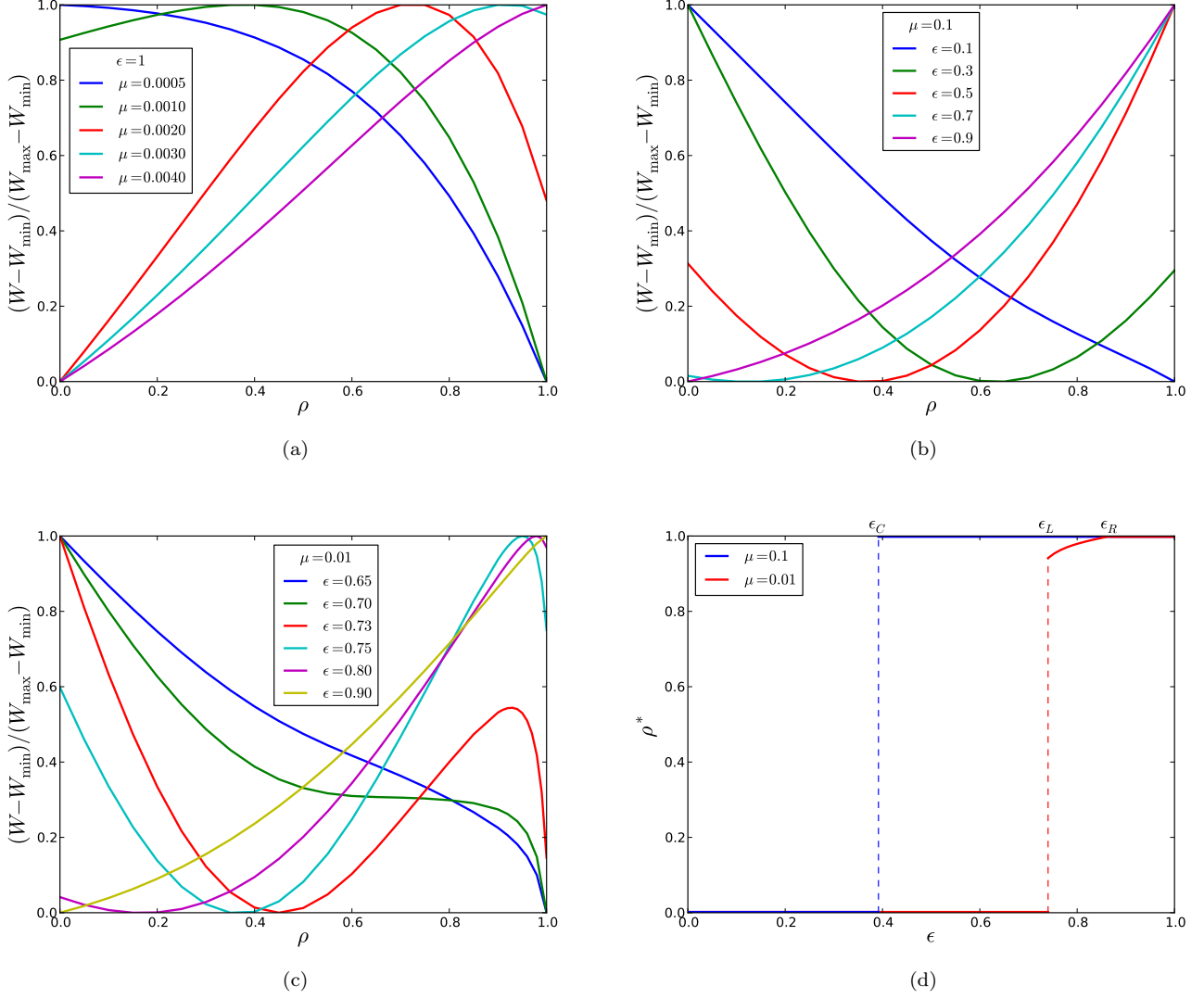


FIG. C1. Asymptotic expansion rate W as a function of phenotype distribution ρ . The birth and death rates of the fast-growing phenotype A and the better-surviving phenotype B are the same as for Figs. 1 and 2 in the main text, i.e., $\beta_A^{(X)} = 2$, $\delta_A^{(X)} = 1$, $\beta_A^{(Y)} = 0$, $\delta_A^{(Y)} = 10$, $\beta_B^{(X)} = \beta_B^{(Y)} = 0.5$, $\delta_B^{(X)} = \delta_B^{(Y)} = 0.1$. The carrying capacity of each local patch is $K = 100$; the sum of the environmental switching rates is $\alpha_X + \alpha_Y = 0.1$. **(a)** the migration rate μ varies, while the environment is X at all times, $\epsilon = 1$, as in Fig. 1. **(b,c)** the environment distribution ϵ varies, while μ is fixed at $\mu = 0.1$ and 0.01 respectively. **(d)** ρ^* as a function of ϵ for μ values used in (c) and (d), corresponding to vertical cross-sections of Fig. 2.

in this example, ρ^* transitions discontinuously from 0 to a positive value ρ_L^* at a certain value ϵ_L , given by $W(0) = W(\rho_L^*)$; yet, as ϵ further increases, ρ^* increases continuously and reaches 1 at another value ϵ_R , as shown in Fig. C1d. In particular, the point (μ_T, ϵ_T) in Fig. 2 is determined by $\rho_L^* = 1$, i.e., when $W(0) = W(1)$ and $W'(1) = 0$. This completes the construction of Fig. 2 in the main text.

Appendix D: More examples on locally fluctuating environments

Here we give a few more distinctive examples of the optimal bet-hedging strategy for a species living in a patchy and locally fluctuating environment. Assume again two possible phenotypes, A and B, and two potential environmental conditions, X and Y. The birth and death rates of each phenotype in a given environment are denoted by $\beta_a^{(\epsilon)}$ and $\delta_a^{(\epsilon)}$, where $a = A, B$, and $\epsilon = X, Y$. The migration rate is μ regardless of the phenotype and the environment. The environment switches from Y to

X and from X to Y with rates α_X and α_Y respectively; thus the stationary distribution of the environment is $p_X = \epsilon = \alpha_X/(\alpha_X + \alpha_Y)$ and $p_Y = 1 - \epsilon$. We assume that a newborn individual, regardless of its parent's phenotype, has probability ρ of having phenotype A, and $(1 - \rho)$ of having phenotype B.

As discussed in the main text, for a fast-growing phenotype A and a better-surviving phenotype B (i.e., $r_A > r_B$ and $q_A > q_B$), there is a range of migration rates μ for which a bet-hedging strategy is optimal even in a constant environment. As an extreme example, consider the case where the fast-growing phenotype in X remains fast-growing in Y, and so does the better-surviving phenotype. In this case, ρ^* as a function of μ is similar to Fig. 1 for both environments, and the phase diagram of $\rho^*(\mu, \epsilon)$ looks typically like Fig. D1a. There is a $0 < \rho^* < 1$ phase that forms a vertical band across the top ($\epsilon = 1$) and bottom ($\epsilon = 0$) borders of the phase diagram. Hence, for any environment distribution ϵ , there is a range of μ values that allow an optimal bet-hedging strategy. Such optimal bet-hedging strategies arise mainly as a result of demographic fluctuations.

Now, consider an opposite situation where the two phenotypes are each suited for a different environment. In particular, each phenotype, A or B, grows normally in one environment, X or Y respectively, yet dies quickly in the other environment. Thus, phenotype A is both fast-growing and better-surviving in environment X, whereas phenotype B is fast-growing and better-surviving in Y. For example, the birth and death rates are such that $\delta_A^{(Y)} \gg \beta_A^{(X)} > \delta_A^{(X)} > \beta_A^{(Y)} = 0$, and similarly $\delta_B^{(X)} \gg \beta_B^{(Y)} > \delta_B^{(Y)} > \beta_B^{(X)} = 0$. We will denote $r_A \equiv \beta_A^{(X)} - \delta_A^{(X)}$, $r_B \equiv \beta_B^{(Y)} - \delta_B^{(Y)}$; $q_A \equiv \delta_A^{(X)}/\beta_A^{(X)}$, $q_B \equiv \delta_B^{(Y)}/\beta_B^{(Y)}$; and $s_A \equiv \delta_A^{(Y)} - \beta_A^{(Y)}$, $s_B \equiv \delta_B^{(X)} - \beta_B^{(X)}$.

The phase diagram of the latter case can be determined, as discussed in the main text, by examining the limits $\epsilon = 0, 1$ and $\mu \rightarrow 0, \infty$. First, when the environment is X or Y at all times, only individuals with the matching phenotype survive; hence we have $\rho^* = 0$ for $\epsilon = 0$, and $\rho^* = 1$ for $\epsilon = 1$, valid for all μ . Then, in the limit $\mu \rightarrow \infty$, the favorable phenotype is the one with a larger average growth rate among

$$\bar{r}_A = \epsilon r_A - (1 - \epsilon)s_A, \quad (D1)$$

$$\bar{r}_B = -\epsilon s_B + (1 - \epsilon)r_B. \quad (D2)$$

Therefore, $\rho^* = 1$ for $\epsilon > \epsilon_c$, and $\rho^* = 0$ for $\epsilon < \epsilon_c$, where $\epsilon_c = \frac{r_B + s_A}{r_A + r_B + s_A + s_B}$. Finally, in the limit $\mu \rightarrow 0$, the asymptotic behavior of ρ^* can be found using an approximation described in Appendix B 3 — when q_A and q_B are small, there is a range of intermediate ϵ values for which a bet-hedging strategy with $0 < \rho^* < 1$ is optimal. This means that, in the phase diagram of $\rho^*(\mu, \epsilon)$, the far left region is horizontally divided into three phases, $\rho^* = 0$, $0 < \rho^* < 1$, and $\rho^* = 1$, as shown in Fig. D1b. The phase boundaries represent discontinuous transitions in ρ^* (see Fig. B1). As μ increases, the two boundaries extend smoothly to the right, and eventually join at a point

(μ_T, ϵ_T). Beyond this point, there is only one boundary separating the $\rho^* = 0$ and $\rho^* = 1$ phases, which becomes asymptotically horizontal as $\mu \rightarrow \infty$.

This phase diagram has a very different character compared to Fig. D1a (or Fig. 2 in the main text). There is no phase transition on the borders of $\epsilon = 0$ or 1, since, for a given environment, one phenotype is advantageous in terms of both a faster growth rate and a lower extinction risk. The existence of an optimal bet-hedging strategy (the $0 < \rho^* < 1$ phase) is mainly due to environmental variations and the fact that different phenotypes are favorable in different environments, just like for a single population in a uniformly fluctuating environment (Sec. D 1). However, in the latter case a favorable bet-hedging strategy always exists for all ϵ , which is not true for the patchy environment, especially for a high migration rate μ .

1. single population in a fluctuating environment

Here we calculate the asymptotic growth rate of a single population in a uniformly fluctuating environment, and derive the optimal bet-hedging strategy. The birth and death rates of the two phenotypes in each environment are the same as for the last example considered above, such that phenotype A is both fast-growing and better-surviving in environment X, and phenotype B is fast-growing and better-surviving in Y. For clarity, here we denote $\beta_A^{(X)} \equiv \beta_A$, $\delta_A^{(X)} \equiv \delta_A$, $\beta_A^{(Y)} \equiv 0$, $\delta_A^{(Y)} \equiv \phi_A$, and $\beta_B^{(Y)} \equiv \beta_B$, $\delta_B^{(Y)} \equiv \delta_B$, $\beta_B^{(X)} \equiv 0$, $\delta_B^{(X)} \equiv \phi_B$.

Similar to Eq. (B11), in the continuous approximation, the population growth in each environment, $\epsilon = X$ or Y, is determined by the matrices

$$\mathbf{H}^{(X)} = \begin{pmatrix} \rho\beta_A - \delta_A & 0 \\ (1 - \rho)\beta_A & -\phi_B \end{pmatrix}, \quad (D3)$$

$$\mathbf{H}^{(Y)} = \begin{pmatrix} -\phi_A & \rho\beta_B \\ 0 & (1 - \rho)\beta_B - \delta_B \end{pmatrix}. \quad (D4)$$

To calculate the asymptotic growth rate, Λ , of the population, we make the approximation that the composition of the population approaches the leading eigenmode of the matrix $\mathbf{H}^{(\epsilon)}$ during each period of time that an environment ϵ lasts. Denote those time periods by $t_n^{(\epsilon)}$, so that they take place in the order $\dots, t_n^{(X)}, t_n^{(Y)}, t_{n+1}^{(X)}, t_{n+1}^{(Y)}, \dots$. The leading eigenmodes of $\mathbf{H}^{(X)}$ and $\mathbf{H}^{(Y)}$ are, respectively,

$$\lambda^{(X)} = \rho\beta_A - \delta_A, \quad \lambda^{(Y)} = (1 - \rho)\beta_B - \delta_B, \quad (D5)$$

$$\boldsymbol{\eta}^{(X)} = \left(\frac{1}{1 - \zeta_B}, 0\right)^T, \quad \boldsymbol{\eta}^{(Y)} = \left(0, \frac{1}{1 - \zeta_A}\right)^T, \quad (D6)$$

$$\boldsymbol{\xi}^{(X)} \equiv (1 - \zeta_B, \zeta_B)^T, \quad \boldsymbol{\xi}^{(Y)} \equiv (\zeta_A, 1 - \zeta_A)^T, \quad (D7)$$

$$\zeta_B \approx \frac{(1 - \rho)\beta_A}{\phi_B} \ll 1, \quad \zeta_A \approx \frac{\rho\beta_B}{\phi_A} \ll 1. \quad (D8)$$

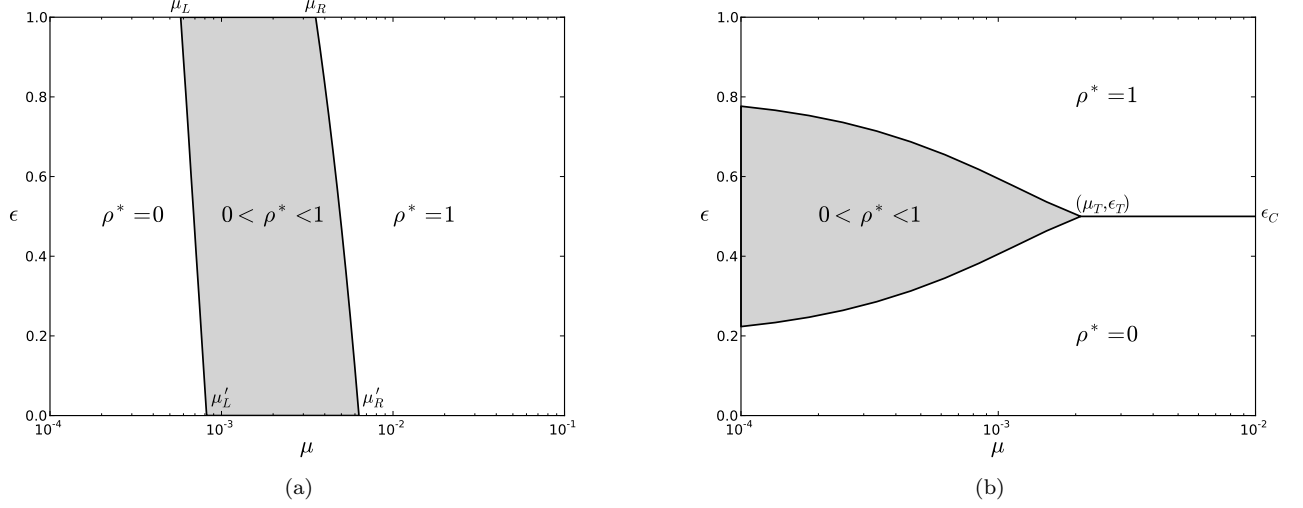


FIG. D1. Phase diagram of the optimal phenotype distribution ρ^* with respect to the migration rate μ and the environment distribution p . Shaded region marks a $0 < \rho^* < 1$ phase in which a bet-hedging strategy offers the maximum asymptotic expansion rate for the species. The carrying capacity of each local patch is $K = 100$; the sum of the environmental switching rates is $\alpha_X + \alpha_Y = 0.1$. **(a)** phenotype A is fast-growing in both environments X and Y, and phenotype B is better-surviving in both X and Y; the birth and death rates are $\beta_A^{(X)} = 2$, $\delta_A^{(X)} = 1$, $\beta_A^{(Y)} = 3$, $\delta_A^{(Y)} = 1.8$, $\beta_B^{(X)} = \beta_B^{(Y)} = 0.5$, $\delta_B^{(X)} = \delta_B^{(Y)} = 0.1$. **(b)** phenotype A offers both a faster growth rate and a lower extinction risk in the environment X, and so does phenotype B in the environment Y; the birth and death rates are $\beta_A^{(X)} = \beta_B^{(Y)} = 5$, $\delta_A^{(X)} = \delta_B^{(Y)} = 1$, $\beta_A^{(Y)} = \beta_B^{(X)} = 0$, $\delta_A^{(Y)} = \delta_B^{(X)} = 50$.

By approximation, the population size N_t grows as

$$N_T \approx \prod_n \left(\boldsymbol{\eta}^{(X)T} \cdot \boldsymbol{\xi}^{(Y)} e^{\lambda^{(Y)} t_n^{(Y)}} \boldsymbol{\eta}^{(Y)T} \cdot \boldsymbol{\xi}^{(X)} e^{\lambda^{(X)} t_n^{(X)}} \right) N_0, \quad (\text{D9})$$

where $T = \sum_n t_n^{(X)} + t_n^{(Y)}$. Hence the asymptotic growth rate is

$$\begin{aligned} \Lambda &= \lim_{T \rightarrow \infty} \frac{1}{T} \log(N_T/N_0) \\ &\approx \lim_{T \rightarrow \infty} \frac{1}{T} \sum_n \left[\lambda^{(X)} t_n^{(X)} + \lambda^{(Y)} t_n^{(Y)} \right. \\ &\quad \left. + \log \left(\boldsymbol{\eta}^{(X)T} \cdot \boldsymbol{\xi}^{(Y)} \right) + \log \left(\boldsymbol{\eta}^{(Y)T} \cdot \boldsymbol{\xi}^{(X)} \right) \right] \\ &= \epsilon(\rho \beta_A - \delta_A) + (1 - \epsilon)((1 - \rho)\beta_B - \delta_B) \\ &\quad + \frac{1}{\tau} \left(\log \frac{(1 - \rho)\beta_A}{\phi_B} + \log \frac{\rho\beta_B}{\phi_A} \right), \end{aligned} \quad (\text{D10})$$

where ϵ is the environment distribution, $\epsilon = \frac{\alpha_X}{\alpha_X + \alpha_Y}$, and τ is the sum of average durations of both environments, $\tau = \frac{\alpha_X + \alpha_Y}{\alpha_X \alpha_Y}$.

Maximizing Λ with respect to ρ yields the optimal phenotype distribution,

$$\rho^* = \frac{2}{2 - \theta + \sqrt{4 + \theta^2}}, \quad \text{where } \theta \equiv \frac{\beta_A}{\alpha_Y} - \frac{\beta_B}{\alpha_X}. \quad (\text{D11})$$

Since $0 < \rho^* < 1$ for all θ , the optimal strategy is always a bet-hedging strategy. For the symmetric case where $\beta_A = \beta_B \equiv \beta$, using $\alpha_X = \epsilon \alpha$ and $\alpha_Y = (1 - \epsilon)\alpha$, we have $\theta = \frac{\beta}{\alpha} \frac{2\epsilon - 1}{\epsilon(1 - \epsilon)}$. Fig. D2 shows ρ^* as a function of ϵ .

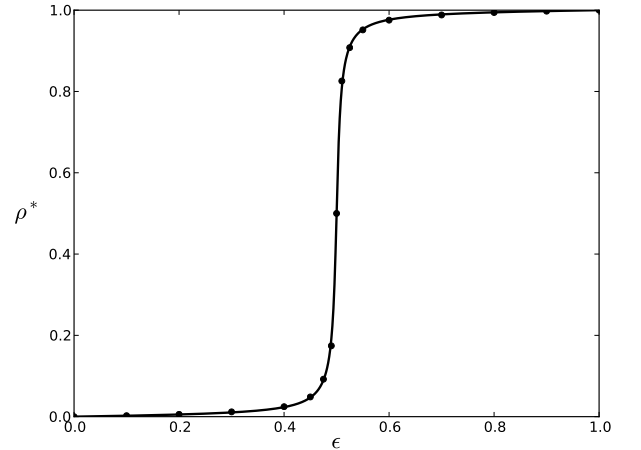


FIG. D2. Optimal phenotype distribution ρ^* with respect to the environment distribution ϵ for a single population in a uniformly fluctuating environment. The birth and death rates of each phenotype and the sum of environmental switching rates are the same as in Fig. D1b. Continuous line is the approximate analytic result according to Eq. (D11); dots are numerically calculated results.

Appendix E: Parent-dependent phenotypic switching

In this appendix we consider a generalization of our model presented in the main text, where an individual's probability of expressing a particular phenotype may depend on the phenotype of its parent. Let a be the phenotype of the parent, and π_{ba} be the probability that the offspring has phenotype b . For two phenotypes A and B, we may parametrize π_{ba} by the phenotypic switching probabilities, $\pi_{BA} \equiv \sigma_A$ and $\pi_{AB} \equiv \sigma_B$, hence $\pi_{AA} = 1 - \sigma_A$ and $\pi_{BB} = 1 - \sigma_B$, where $0 \leq \sigma_a \leq 1$.

Instead of Eq. (8) in the main text, the birth process is now described by:

$$\mathbb{I}_i^a + \emptyset_i \xrightarrow{\pi_{ba} \beta_a / K} \mathbb{I}_i^a + \mathbb{I}_i^b, \quad (\text{E1})$$

whereas the death and migration processes are the same as in Eqs.(9,10). Accordingly, for the patch dynamics, Eqs. (11,12) are replaced by

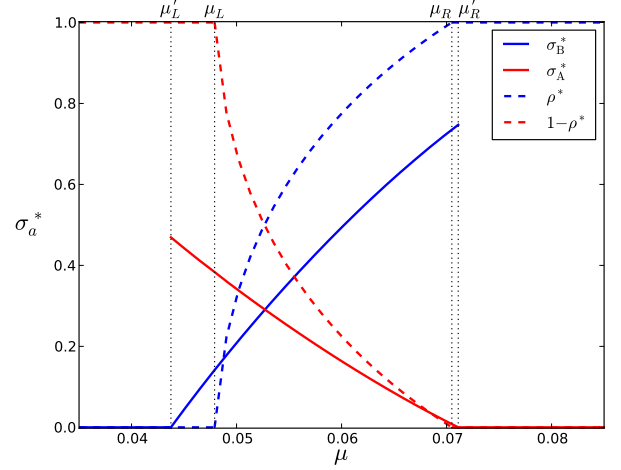
$$P_{n,l} \xrightarrow{\eta_{nl}} P_{n+1,l+1}, \quad (\text{E2})$$

$$P_{n,l} \xrightarrow{\theta_{nl}} P_{n+1,l}, \quad (\text{E3})$$

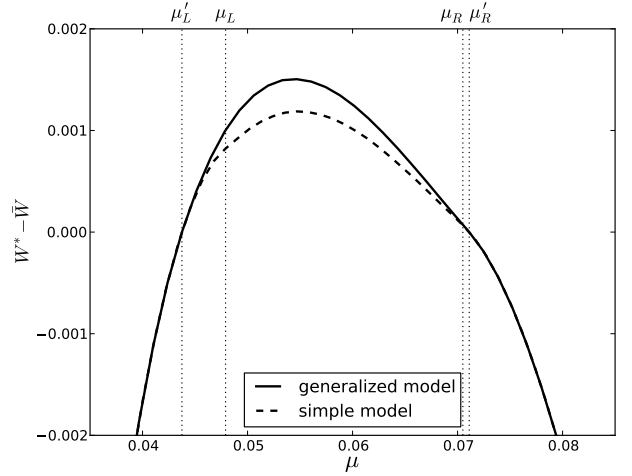
where the new rate constants are $\eta_{nl} = (1 - \sigma_A)\beta_A l(1 - n/K) + \sigma_B\beta_B(n - l)(1 - n/K)$, and $\theta_{nl} = \sigma_A\beta_A l(1 - n/K) + (1 - \sigma_B)\beta_B(n - l)(1 - n/K)$. The asymptotic expansion rate W can be calculated in the same way as in Sec. B2, by replacing $\rho\beta_{nl}$ with η_{nl} and replacing $(1 - \rho)\beta_{nl}$ with θ_{nl} .

In this generalized model, we maximize W with respect to both σ_A and σ_B . Their optimal values, σ_A^* and σ_B^* , are plotted as functions of the migration rate μ in Fig. E1a. There is a lower bound, μ'_L , below which $\sigma_B^* = 0$ and σ_A^* can take any values between 0 and 1. It means that, for such very low migration rates, offspring of parental phenotype B never switch to phenotype A, and this “pure B” subpopulation contributes the maximum asymptotic expansion rate for the species; meanwhile, there may coexist a nonzero subpopulation of phenotype A if $\sigma_A < 1$, yet their number would be subdominant and does not affect the asymptotic expansion rate. Similarly, for migration rates above an upper bound, μ'_R , the optimal phenotypic switching probabilities are $\sigma_A^* = 0$ and $\sigma_B^* = \text{any value between 0 and 1}$. It means that, for sufficiently high migration rates, the optimal strategy for the species is to have a dominant “pure A” subpopulation that never switch to phenotype B.

Note that the simple, parent-independent, model presented in the main text corresponds to $\sigma_A = 1 - \rho$ and $\sigma_B = \rho$, satisfying $\sigma_A + \sigma_B = 1$. The generalized model relaxes the last constraint by letting σ_A and σ_B vary independently. It can be seen from Fig. E1a that their optimal values do not satisfy the constraint. For comparison, the optimal value ρ^* obtained for the simple model is also shown in the figure, which satisfies $0 < \rho^* < 1$ for μ between two bounds μ_L and μ_R . Since the generalized model is less constrained, one expects the maximum asymptotic expansion rate W^* to be no less than that



(a)



(b)

FIG. E1. Generalized model with parent-dependent phenotypic distribution. The birth and death rates of each phenotype are $\beta_A = 3$, $\delta_A = 2$, and $\beta_B = 1$, $\delta_B = 0.25$; the carrying capacity of each local patch is $K = 100$. (a) Optimal phenotypic switching probabilities σ_a^* ($a = A, B$) with respect to the migration rate μ . For comparison, dashed lines show the optimal phenotype distribution ρ^* and $(1 - \rho^*)$ given by the simple parent-independent model presented in the main text. (b) Maximum asymptotic expansion rate W^* versus migration rate μ in both the simple (dashed curve) and the generalized (solid curve) models. For clear comparison, we subtracted a same term $\bar{W}(\mu) \equiv \frac{\mu'_R - \mu}{\mu'_R - \mu'_L} W^*(\mu'_L) + \frac{\mu - \mu'_L}{\mu'_R - \mu'_L} W^*(\mu'_R)$ from each curve.

in the simple model. This is indeed the case, as illustrated in Fig. E1b. The two curves coincide at values of the migration rate below μ'_L and above μ'_R , because in those cases only one phenotype, B and A respectively, completely dominates the population in both the simple and the generalized models.